Hindawi
Geofluids
Volume 2022, Article ID 3633047, 17 pages
https://doi.org/10.1155/2022/3633047

Review Article

Occurrence, Genesis, and Significance of Analcime in Fine-Grained Sedimentary Rocks

Junran Wang,[1] **Chao Liang**,[1,2] **Yingchang Cao**,[1] **and Yu Tian**[1]

[1]*Key Laboratory of Deep Oil and Gas, China University of Petroleum (East China), Qingdao 266580, China*
[2]*Shandong Provincial Key Laboratory of Depositional Mineralization & Sedimentary Mineral, Shandong University of Technology, Qingdao 266590, China*

Correspondence should be addressed to Chao Liang; liangchao0318@upc.edu.cn

Received 18 September 2021; Revised 22 December 2021; Accepted 25 January 2022; Published 12 March 2022

Academic Editor: Hasan N. Al-Saedi

Natural analcime, an aluminosilicate mineral with multiple genetic mechanisms, widely occurs in fine-grained sedimentary reservoirs rich in oil and gas. Researchers have discussed the source and formation mechanism of reservoirs and the influence of morphology formation, occurrence characteristics associated with minerals, geochemical data, and Si/Al ratio on reservoir properties. The occurrence location, particle size, automorphism, purity, and fracture development can indicate the source of analcime macroscopically. The correlation between the enrichment of associated minerals and the content of analcime indicates that the associated mineral assemblage or correlation provides a material source for the formation of analcime or effectively improves the formation environment. Geochemical data are often used to identify analcime related to primary magmatic crystallization and hydrothermal processes. The genetic source grouping scheme based on the Si/Al ratio, which is a traditional means to identify the source of analcime, has been widely used in the research on analcime. After more than 200 years of study, research has shown that analcime distributed in fine-grained sedimentary rocks was mainly formed by burial alteration of volcanic materials (V-type analcime), conversion of nontuffaceous materials (N-type analcime), hydrothermal deposition mineralization (H-type analcime), and precipitation directly from an alkaline lake or pore water (P-type analcime). Based on reservoir properties, analcime that formed before the organic acid release stage of source rocks can effectively improve the porosity through precipitation–dissolution mechanisms after the release of massive organic acid, whereas the cementation formed by the transition of the fluid from acid to alkaline during the intermediate diagenetic stage would reduce porosity to some extent.

1. Introduction

In terms of analcime, an important natural aluminosilicate mineral, Bradley published an article in the journal "Science" and recorded authigenic analcime from tuff and oil shale in the Eocene Green River Formation of North America [1]. Discussion on the occurrence, source, and formation mechanism of analcime has continued for nearly a century since that report. Various zeolite minerals such as mordenite, clinoptilolite, natrolite, analcime, heulandite, and laumontite have been discovered in low-grade metamorphic and sedimentary rocks [2–5].

Analcime is widely distributed in tuff, biochemical rocks, and clay rocks, with various occurrence forms, sources, and multiple formation mechanisms. Based on these characteristics, the coexistence of different types of analcime is common under the influence of complex sedimentation, burial, and diagenesis. In the Rocky Brook Formation of the Deer Lake Basin, USA, the analcime formed by the interaction between water and clay minerals and that formed by direct precipitation coexist in the form of pore filling and dispersed micritic particles under the control of saline-alkaline lake or pore water [6, 7]. In the Shahejie Formation of the Bohai Bay Basin, China, laminar analcime, fracture-filling analcime, and nodular analcime coexist under the influence of the hydrothermal fluid and high-alkaline water [8, 9].

Analcime is closely related to volcanic materials in common. In saline and alkaline lakes rich in volcanic materials, precursor minerals are formed by the alteration of volcanic siliceous glass and eventually transform into

analcime [1, 10]. With improvements in experimental instruments and research methods, the understanding of these precursor minerals has been constantly improved by various silicate–aluminate minerals, including alkaline zeolite [11], silicate–aluminate gel [12, 13], clay minerals [14], feldspar [15], and minerals with properties similar to these minerals. In sedimentary areas lacking pyroclastic material, analcime is mainly formed via three mechanisms: (1) conversion of nontuffaceous materials (clay, feldspar, and alkaline zeolite) [12, 16–20]; (2) hydrothermal deposition mineralization [21–25]; and (3) precipitation directly from an alkaline lake or pore water [7, 26–28]. To distinguish analcime formed under different mechanisms, researchers summarized the characteristics of the morphology, associated minerals, geochemistry, and Si/Al ratio.

In the past 30 years, analcime has proved to be an important component of high-quality oil and gas reservoirs [29]. Domestic and foreign scholars began to focus on transforming the reservoir by analcime during diagenetic evolution to explore and discuss the effects of improving the porosity from both positive and negative perspectives. The previous work is systematically summarized and typical research cases are compared to supplement the analysis of the occurrence characteristics, formation mechanism of analcime in fine-grained sedimentary reservoirs, and changes in reservoir properties caused by analcime.

2. Analcime Characteristics

Analcime is a sodium-rich aluminosilicate mineral widely distributed in sedimentary rocks, which has an ideal chemical formula of $Na_{16}Al_{16}Si_{32}O_{96}{\bullet}16H_2O$ [2]. The structure of analcime is equiaxially homogeneous, hexagonal, or octagonal and colorless with low-negative projections under single-plane polarized light and shows full extinction under orthogonal light. The crystal structure comprises silica–aluminate lattice, channels, voids, and cations [30]. Owing to the influence of host-rock composition, hydrochemical conditions, salinity, pH, burial depth, and diagenetic stage, the structural properties and chemical composition of natural analcime will deviate from the ideal molecular formula to some extent ($Na[AlSi_{2-2.8}O_{6-7.6}]_6{\bullet}1{-}1.3H_2O$) [2]. At present, domestic and foreign scholars judge the source of analcime mainly from four aspects: (1) occurrence form [31–33], (2) associated minerals and their relative contents [12, 18, 19], (3) geochemical characteristics [22, 23, 34], and (4) Si/Al ratio [3, 26, 35].

2.1. Structural Properties. Analcime is generated by a TO_4 tetrahedron linked to adjacent self-similar units that share O_2 in the corner of the tetrahedron, in which T is most commonly Si or Al [29, 36]. In the process of secondary construction, the basic crystal structure comprises six-membered or four-membered ring structures (Figure 1). Under the influence of temperature, pressure, and cationic displacement, the symmetry, volume space change, and structure become more complex and diverse.

Due to the high structural openness of analcime, Na is commonly replaced by K, Ca, and Mg and the substitution rate in some samples can reach 20%. Compared with the structure of Si–O–Si, a Si–O–Al skeleton is more likely to rupture in an acidic environment. Therefore, analcime is extremely unstable under the action of acidic fluid [37, 38].

2.1.1. Pressure. In the burial process, the environmental pressure increases with the burial depth, the crystal structure changes continuously within a certain range of pressure, and the volume changes discontinuously. High-pressure X-ray powder diffraction experiments show that the phase transformation interface of analcime exists at 8 kbar (Yoder and Weir, 1960), and differential thermal analysis shows that the value of dP/dT was 0.057 kbar/°C [39].

Based on these results, researchers have conducted further studies on the structural phase transformation of analcime with an increase in pressure. The phase transformation experiment of analcime in a high-pressure environment conducted by Robert et al. (1979) [40] showed that under pressure conditions of 0–25 kbar, analcime experienced four structural stages and there are two discontinuous surfaces of volume change (Figure 2). When the pressure is more than 4 kbar, the cell changes from an orthogonal structure to a C-centered monoclinic structure, in which the first discontinuity of volume change is experienced at approximately 8 kbar and the crystal structure transformation is completed at 12 kbar. When the pressure exceeds 12 kbar, the cell changes from C-centered monoclinic structure to triclinic structure, transforms completely at 19 kbar, and undergoes a second discontinuity of volume change. From 19 to 25 kbar, analcime exists stably in the triclinic structure and its structure will not considerably change under further pressurization [40].

2.1.2. Temperature. Temperature affects both the rate of reaction and the type of zeolite minerals formed. In general, the reaction rate increases with an increase in temperature and water-deficient zeolite is more stable than in water-rich zeolite at high temperatures. Iijima (2001) analyzed borehole temperatures of oil fields in Japan and suggested that fresh glass transforms to clinoptilolite or mordenite at temperatures of 41–55°C and clinoptilolite and mordenite are altered to analcime at 84–91°C and form albite at about 120°C (Figure 3) [41–44].

Owing to their scarcity and tiny sizes, conducting fluid inclusion thermometry analysis for sedimentary rocks with authigenic analcime is difficult [5], and dividing the formation intervals of analcime only on the basis of temperature is not suitable as well. In the fluid phase environment, the change in temperature has a certain effect on the precipitation of analcime by influencing the concentrations of the ions (Figure 4) [45, 46].

2.2. Occurrence Characteristics. Occurrence characteristics include location, particle size, idiomorphic degree, purity of the crystal, and fracture development. These features can

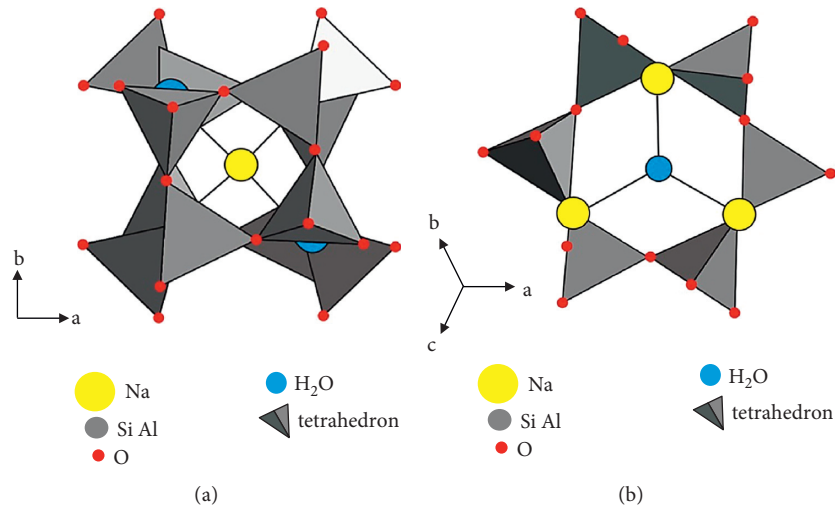

Figure 1: Crystal structure of analcime (Armbruster and Gunter, 2001; Xiao, 2014) [30, 36]. (a) Four-membered ring structure. (b) Six-membered ring structure.

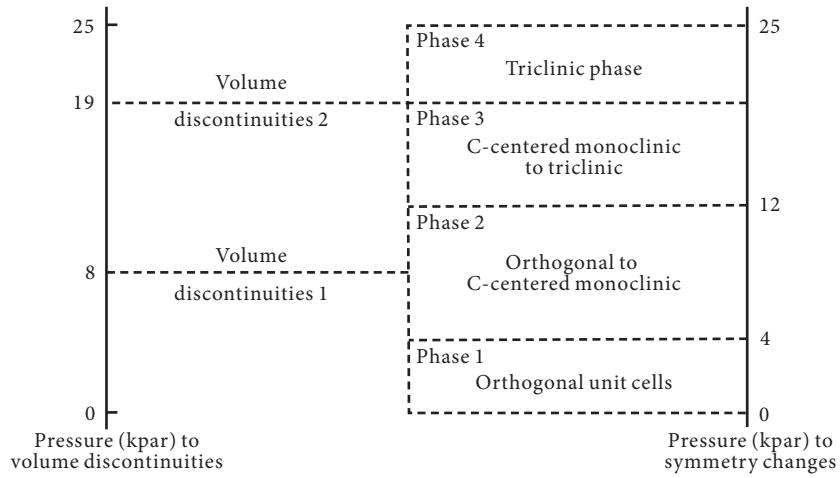

Figure 2: The structural variation of analcime with pressure.

indicate the source of analcime on a macroscale. Analcime that crystallized directly from magma usually appears phenocrystalline with smooth and clean surfaces, in which micropores and cracks are rare (Figures 5(a) and 5(b)) [32]. Analcime grains formed by the transformation of the host-rock minerals (volcanic material, leucite, nepheline, feldspar, and other zeolite group minerals) usually possess irregular granularity. Their crystal surfaces are rough and prone to develop cracks and micropores (Figures 5(c) and 5(d)) [47]. Analcime formed by hydrothermal filling crystallization is often found in cracks and pores in veins (Figures 5(e) and 5(f)). Analcime formed from a silica aluminous gel is usually filled in the intergranular spaces or fissures as cement (Figures 5(g)–5(i)) [28, 33].

2.3. Associated Minerals. Common analcime-associated minerals include volcanic glass, alkali feldspar, alkaline zeolite, clay minerals, and carbonate minerals, followed by organic matter and oxides, such as pyrite and rhodochrosite. When there is a correlation between the enrichment of an associated mineral and the content of analcime, there exists an obvious conversion to analcime under the microscope. Correlation and conversion are considered to provide a material source for the formation of analcime or effectively improve the formation environment of analcime. Volcanic siliceous glass is generally considered to be the basis for precursor minerals. The high activity of silicon provides favorable conditions for forming analcime. In the Green River Formation in Utah, Miocene strata in Central Anatolia, and Pleistocene strata in the Lake Lewis Basin [10, 12, 50], clay minerals and albite have been proven to be the precursor minerals of analcime. In the fine-grained sedimentary rocks of the Ek_2 Formation in the Cangdong Sag, Huanghua Depression, the contents of analcime and clay minerals have a negative correlation along the longitudinal direction [19]. In the Lucaogou Formation of the Jimusar Sag, Junggar Basin, the content of analcime

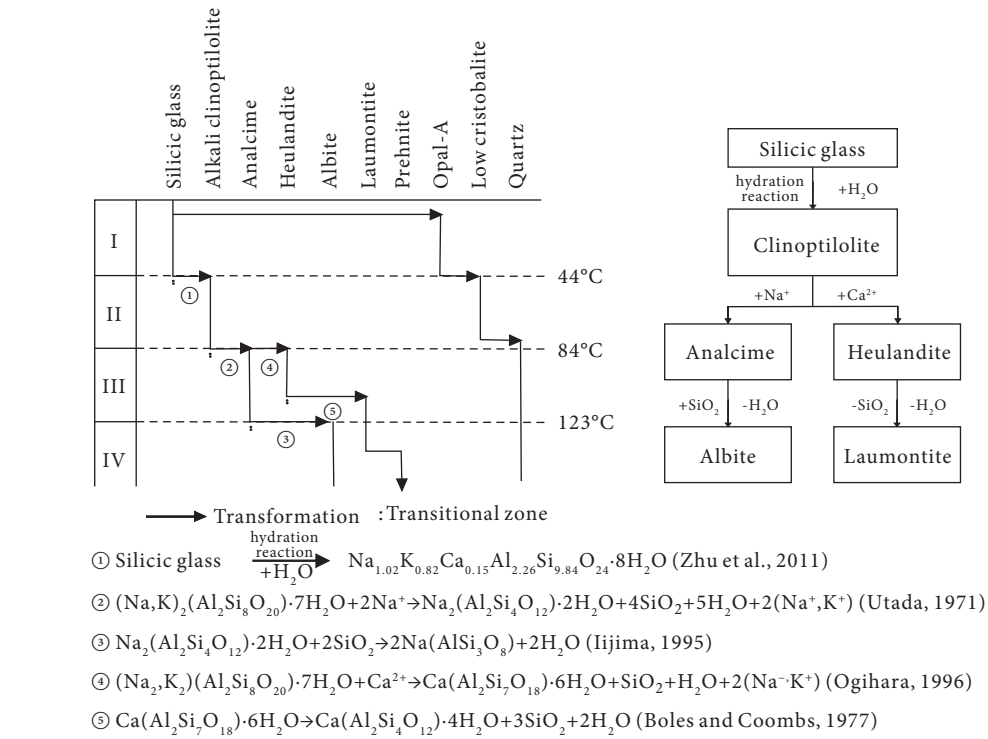

Figure 3: Present-day borehole temperatures at boundaries between zeolite zones in the Japanese islands (modified according to Lijima, 2001) [42].

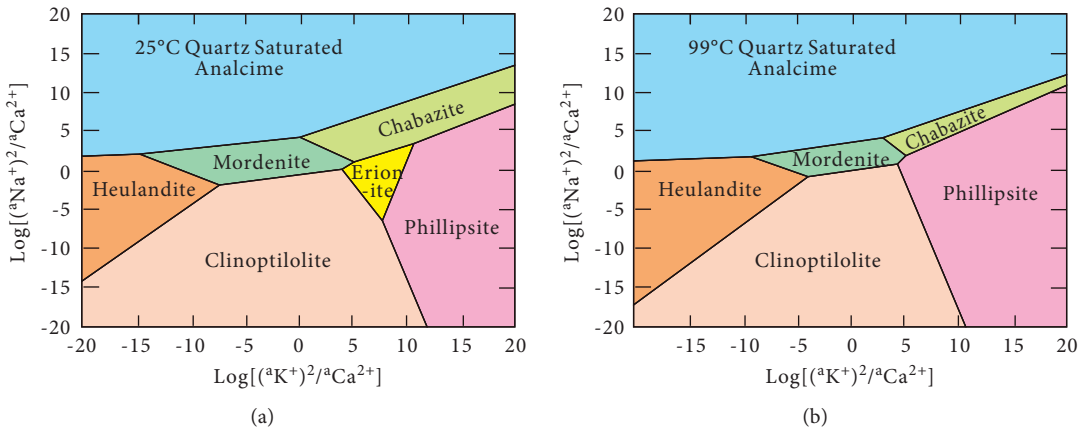

Figure 4: The difference in $\log[(^aK^+)^2/^aCa^{2+}]$ versus $\log[(^aNa^+)^2/^aCa^{2+}]$ of zeolite phases under quartz saturation at different temperatures (modified according to Chipera et al., 2008) [45]. (a) The difference of $\log[(^aK^+)^2/^aCa^{2+}]$ versus $\log[(^aNa^+)^2/^aCa^{2+}]$ of zeolite phases under quartz saturation at 25°C. (b) The difference of $\log[(^aK^+)^2/^aCa^{2+}]$ versus $\log[(^aNa^+)^2/^aCa^{2+}]$ of zeolite phases under quartz saturation at 99°C.

increases with the decrease in alkali feldspar [20]. In the lacustrine exhalative rocks of the Xiagou Formation in the Jiuxi Basin, analcime is closely associated with dolomite and iron dolomite, which supports the hypothesis of hydrothermal deposition mineralization of analcime [34, 51].

2.4. Geochemical Characteristics. Geochemical data are often used to identify analcime related to primary magmatic crystallization and hydrothermal processes. The distribution patterns and enrichment anomalies of elements can indicate the original source of minerals to a certain extent. In the lacustrine exhalative rocks of the Xiagou Formation in the Jiuxi Basin, the distribution patterns of rare Earth elements and anomaly characteristics of δCe and δEu between the source rock of analcime and contemporaneous basalt act in extremely similar ways. This suggests that the two may have the same origin [34]. In addition, previous studies have shown that the host rocks of hydrothermal deposition mineralization of analcime associated with dolomite in high-salinity alkaline lake basins are usually characterized via enrichment in light rare Earth elements and ^{13}C and depletion in heavy rare Earth elements and ^{18}O [22, 23].

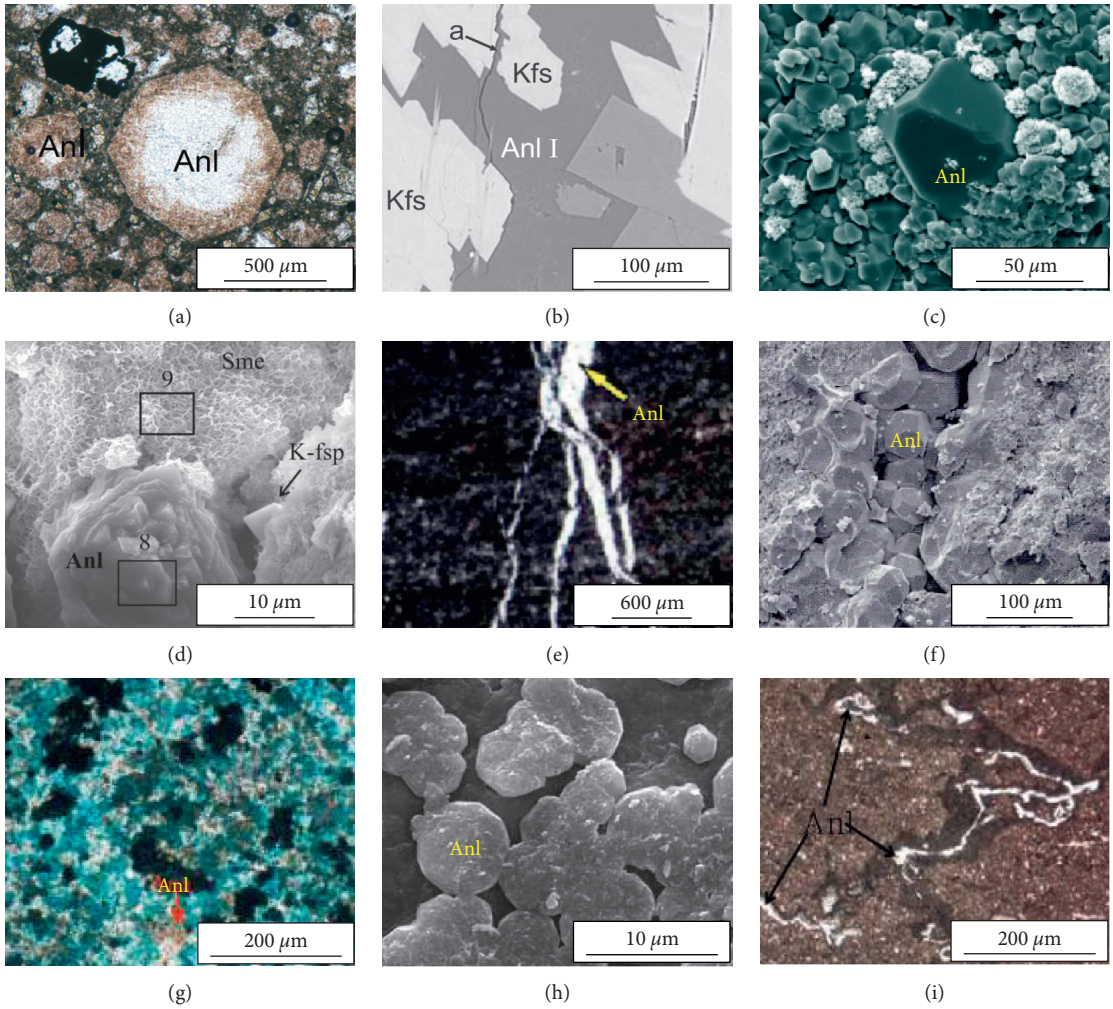

Figure 5: Occurrence forms of analcime. (a) Micrographs of euhedral and nearly rounded analcime from analcime-bearing volcanic rocks. (b) Magmatic texture comprised K-feldspar, albite (Ab), and analcime (Anl) [48]. (c) The crystalline tuff matrix is transformed into analcime [23]. (d) Growth of authigenic analcime from volcanic material [18]. (e) Micritic dolomite, in which fractures are partially filled with analcime [8]. (f) Micritic dolomite, in which fractures are filled with euhedral analcime [49]. (g) Analcime gel (yellow, indicated by red arrow) is filled in between micritic ankerite particles (green–blue) [23]. (h) Subhedral globules of analcime gel, with isolated euhedral analcime crystals occupying pore spaces in the center left and upper right [12]. (i) Liquefaction veins are filled with analcime cement in massive dolomite [19].

2.5. Si/Al Ratio. Coombs and Whetten (1967) [3] summarized the chemical compositions of different genetic analcimes and considered that the source and genetic information of analcime can be obtained through the Si/Al ratio. They put forward a three-type grouping scheme with the function of indicating the genetic source, as follows: (1) high silica analcime derived from siliceous volcanic glass (Si/Al: 2.52–2.79): the analcimes from Yavapai, Arizona [29, 52, 53], analcimes of the Tower Sandstone of the Green River Formation formed by the reaction of "sodium-rich alkaline lake water with volcanic glass [2, 54], and analcimes from a thin bed near the top of the Wilkins Peak Member of the Green River Formation underlying the Tower Sandstone [35] (Teruggi, 1964); (2) medium-silica analcime formed by modification of aluminosilicate minerals during burial (Si/Al: 2.52), which may be formed by metamorphism or generated in the early diagenetic stage to persist under burial metamorphism. Typical examples include analcime distributed in of the Murihiku Super Formation in southern New Zealand [55], Carboniferous tuffaceous sandstone and rhyolite in southwestern New South Wales; (3) low-silica analcime formed by direct precipitation of high-salinity alkaline lake water or reaction with other sediments (Si/Al: 2.07–2.28), which often coexists with chemically deposited dolomite and has poor thermal stability. Typical examples include analcime distributed in the mudstone of the Lockatong Formation [56], Popo Agie Formation [57, 58], and Kongdian Formation in the Cangdong Sag of the Bohai Bay Basin [19]. However, it is not appropriate to classify analcime only based on the Si/Al ratio, especially in organic rich source rocks. Wide formation temperature range, diverse precursor minerals, and the instability in the acidic environment make the formation and dissolution of analcime almost cover the whole early diagenetic stage and

intermediate diagenetic stage, and its components change obviously in the complex diagenetic process. Therefore, in most cases, the Si/Al ratio could not directly indicate its formation environment but play a macro indicating role.

3. Analcime Genetic Types in Fine-Grained Sedimentary Rocks

Fine-grained sedimentary rocks, commonly comprising terrigenous clastic, biogenic particle, and chemical precipitation particle, form a monolayer or mixed layer. The particle size, which is less than 62 μm, fluctuates between clay and silt levels. The main components include terrigenous clastic materials, clay minerals, carbonates, calcium oxides, halides, organic matter, and siliceous biological particles [59–61]. In 1989, Luhr and Kyser classified analcime into five types according to its genesis (Table 1); this classification scheme has been recognized and used by most scholars. However, the classification is difficult to support a more detailed discussion for analcime distributed in fine-grained sedimentary rock. Therefore, analcime is reclassified according to the differences of genetic mechanism for review and discussion in this article (Table 1).

As a favorable mineral to improve reservoir properties, the formation pattern of analcime has a high-reference value for the study of fine-grained reservoirs. Thus far, domestic and foreign scholars have reported several cases of analcime being distributed in fine-grained sedimentary rocks of lake basins (Table 2).

Different lithofacies control the formation of analcime. Generally, mudstone, siltstone, and tuff provide a necessary source of siliceous alumina materials. For limestone and dolomite, calcite and dolomite could not exist as the precursor minerals of analcime, but they provide a favorable environment for analcime precipitation, especially in adjusting the fluid properties. Combined with the information on occurrence forms, associated minerals, and geochemical analysis results, the formation mechanism of analcime can be divided into four types: (1) burial alteration of volcanic materials (V-type); (2) conversion of nontuffaceous materials (N-type); (3) hydrothermal deposition mineralization (H-type); (4) precipitated directly from an alkaline lake or pore water (P-type).

3.1. Burial Alteration of Volcanic Materials: V Type. Analcime formed by the burial alteration of volcanic material is often distributed in sedimentary lake basins with frequent volcanic activities. Pyroclastic materials enter the lake basin through transport in water or the atmosphere and form silica-rich sediments. Under the action of saline-alkaline lake water, the pyroclastic materials are transformed into precursor minerals (clay minerals, alkaline feldspar, and alkaline zeolite), which are further transformed into analcime (Figure 6).

In a closed lake basin, horizontal changes in salinity and alkalinity cause the sediment species to be distributed in circular zones. In the low-salinity lake margin, developing mordenite and alkaline-poor zeolites is simple; toward the center of the lake, the zeolite species transition to high-alkaline zeolite represented by analcime as the salinity and alkalinity increase; in the center of the lake, the salinity is highest and alkaline feldspar is developed [2, 17] (Figure 6).

Tuffaceous material is one of the most important indicators to identify analcime of volcanic origin, which is usually consistent with the distribution of analcime. In the matrix of the tuffaceous layer and surface of siliceous debris, the conversion to analcime is common (Figures 7(a)–7(c)).

Remy and Ferrell (1989) summarized previous views on the origin of analcime in the lacustrine sedimentary rocks of the Green River Formation (Table 3). This study shows that analcime formed by the transformation of volcanic materials is always an important component mineral in the Green River Formation.

3.2. Conversion of Nontuffaceous Materials: N Type. Analcime formed via nontuffaceous transformation is widespread in the tuff-poor fine-grained sedimentary rocks of sodium-rich alkaline lake basins. The lack of pyroclastic deposits precluded the possibility that the precursor minerals were derived from volcanic glass. In this case, the conversion of clay and feldspar minerals became the main mode of analcime formation. Typical examples here include analcime distributed in the Es_3 Formation in the Beitang Sag [8]; Ek_2 Formation in the Cangdong Sag [19]; Green River Formation in Utah, Miocene unit in Central Anatolia, and Pleistocene strata in the Lake Lewis Basin [10, 12, 18, 50]. This type of analcime is mainly distributed as dispersible micritic particles in the argillaceous layer or as intercalations comprising carbonate and clay minerals. Secondary occurrences are in the form of cement in sandy particles and fractures. Under the action of low concentrations of Si, silica–aluminate phase minerals tend to convert from stable to substable states, which makes it difficult for clay minerals (particularly montmorillonite and kaolinite) and alkali feldspar (e.g., sodium feldspar) to exist stably in a silica-poor system. Being in this state for a long time, self-formation of analcime would be poor and even transform into amorphous colloids. Based on this observation, large amounts of Na, Si, and Al are released, forming the basis for analcime formation.

3.2.1. Clay Mineral Transformation. The conversion of clay minerals to analcime has been reported several times in the lacustrine sedimentary basins with inadequate volcanic materials. Analcime is mainly distributed in laminar, directional lenses (Figure 8(a)) and dispersed as independent micritic particles (Figure 8(b)). When distributed in layers, analcime is often interbedded with carbonate and mixed layers (Figures 8(c)–8(f)). In the process of forming analcime, Na^+, Al^{3+}, and Si^{4+} are released to react with alkaline lake or pore water. The infiltration of alkaline water changes the salinity; clay particles are prone to flocculation or experience a volume change under the influence of the salinity change. The clay flocculants provide the basis for the formation of directional lenticular analcime aggregates; the shrinkage of the volume provides favorable conditions for

Table 1: Classification scheme of analcime.

Classification scheme of analcime			
Luhr and Kyser, 1989		This article	
Formation mechanism	Symbol	Formation mechanism	Symbol
Produced by magnetic crystallization	P/I	Burial alteration of volcanic materials	V
Produced by ion exchange of leucite nepheline or zeolite	X/L	Conversion of nontuffaceous materials	N
Produced by hydrothermal action	H	Hydrothermal deposition mineralization	H
Produced by diagenesis	S	Precipitated directly by alkaline ake or pore water	P
Produced by buried metamorphism	M		

Table 2: Analcime in lacustrine fine-grained sedimentary rocks.

Basin	Formation	Age	Lithology	Occurrence	Proposed origin	Type model	References
Deer Lake Basin	Rocky Brook Formation	/	Fine-grained sandstones, dolomitic mudstone, and limestone	Pore/crack filling and disperse individual micrite particles	Direct precipitation of lake or pore water; clay minerals transformation	P-type N-type	Gall and Hyde [7]
Lake Lewis Basin, Central Australia	/	E_2	Siltstone and tuffs	Pore/crack filling and intergranular crystallization	Clay minerals transformation; precipitated from sodium aluminosilicate gels	P-type N-type	English [12]
South-central Uinta Basin, Utah	Green River Formation	E	Mudstone and siltstone	Fine-grained disseminated crystals and coarser-grained pore-filling cement	Direct precipitation of lake or pore water; clay minerals transformation	P-type N-type	Remy and Ray [10]
Maíz Gordo Basin Argentina	Maíz Gordo Formation	E_2-E_1	Siltstone, carbonate mudstone, and silicified tuff	Pore/crack filling, vein-shaped, and globular crystals	Direct precipitation of lake or pore water; clay minerals transformation;	P-type N-type	Campo et al., [17]
Lake Bogoria Basin, Kenya Rift Valley	/	Q_3	Siltstone and mudstone	Pore/crack filling and intergranular crystallization	Direct precipitation of lake or pore water; clay minerals transformation; precipitated from sodium aluminosilicate gels	P-type N-type H-type	Renaut [62]
Jimsar Sag Junggar Basin	Lucaogou Formation	P_2	Sedimentary tuff, carbonate tuff, and tuffaceous dolomite	Lamellar, granular, and vein-shaped	Alkaline feldspar and montmorillonite; transformation; volcanic material alteration	N-type V-type	Ma et al., [20] Li et al., [23]
Santanghu Basin	Lucaogou Formation	P_2	Argillaceous dolomite, dolomitic mudstone, micrite, and dark mudstone	Lamellar and amorphous gelatinous	Hydrothermal jet mineralization	H-type	Li et al., [23]
Cangdong Sag Bohaiwan Basin	Kongdian Formation	E_2	Mixed fine-grained, Sedimentary rocks, and tight sandstone;	Lamellar, pore/crack filling, and vein-shaped	Direct precipitation of lake or pore water; clay minerals transformation	P-type N-type	Zhang et al., [19]

further infiltration of alkaline lake water and the formation of analcime. The main clay conversion reactions are as follows:

$$Na_{0.33}Mg_{0.33}Al_{1.67}Si_4O_{10}(OH)_2 + 4.68OH^- + 2H_2O \longrightarrow 0.33Na^+ + 0.33Mg^{2+} + 1.67Al(OH)_4 + 4HSiO_3^-, \quad (1)$$

$$Na^+ + Al(OH)_4 + 2HSiO_3^- \longrightarrow NaAlSi_2O_6 + 2OH^- + H_2O, \quad (2)$$

$$Al_2Si_2O_5(OH)_4\,(\text{kaolinite}) + Na_2CO_3 + 2SiO_2 + 2H_2O = Na_2Al_2Si_4O_{12} \cdot 4H_2O + CO_2, \quad (3)$$

$$Na_x(H_2O)4\{Al_{2-x}Mg_x[Si_4O_{10}](OH)_2\}\,(\text{montmorillonite}) + Na^+ = Na_2[AlSi_2O_6]_2 \cdot 2H_2O + H^+. \quad (4)$$

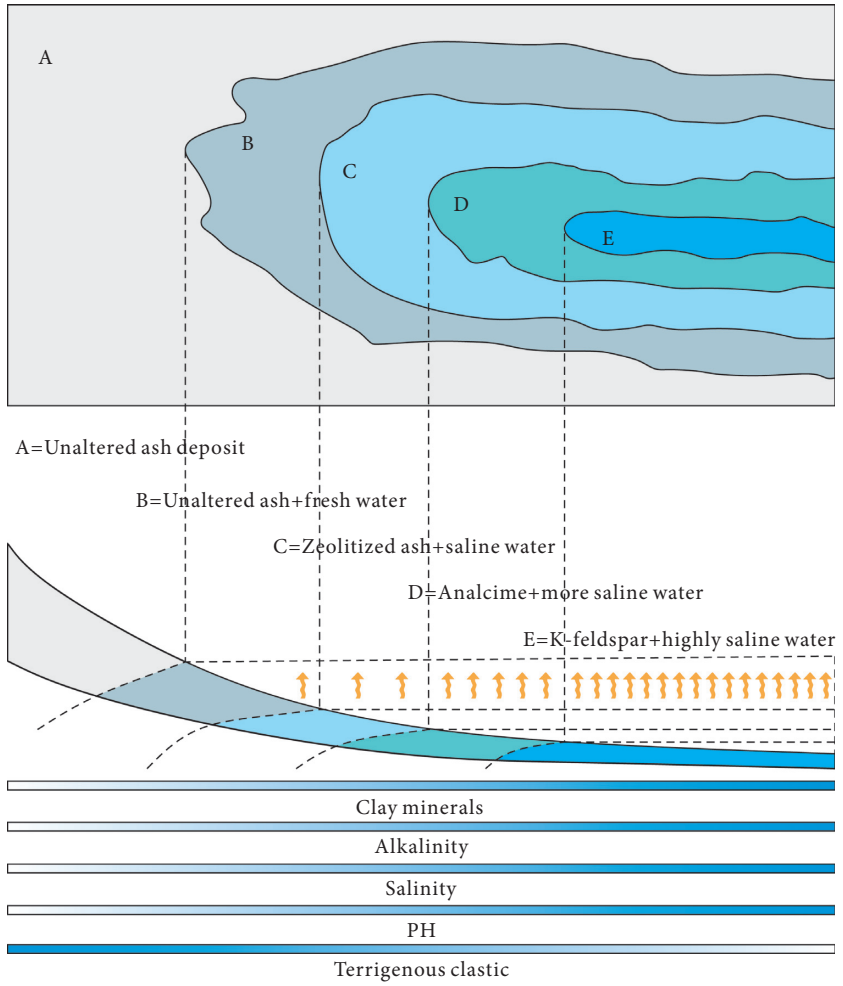

Figure 6: Distribution of authigenic mineral zones in the saline, alkaline playa-lake system (modified according to Langella et al., 2001).

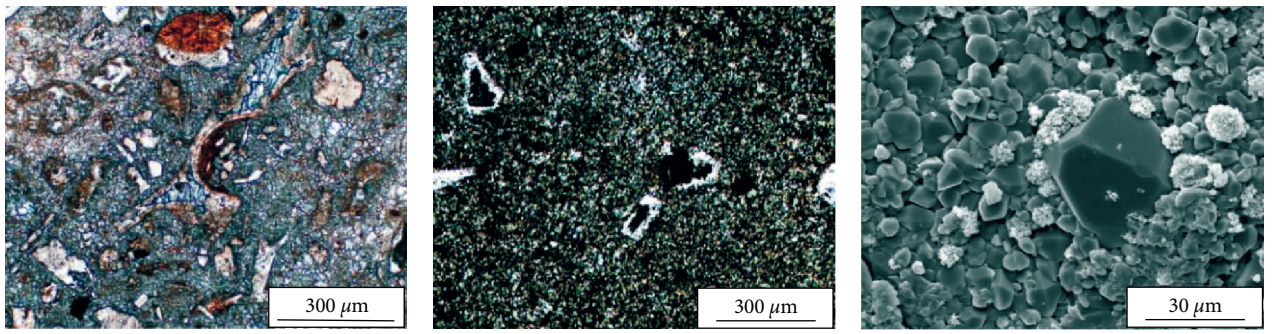

Figure 7: Analcime transformed from volcanic material [23]. (a) In vitreous clastic tuff, the vitreous clastic surface and matrix all transform into analcime. (b) Clastic tuff. (c) Crystalline tuff, in which the matrix is transformed to euhedral granular analcime.

Table 3: Reported occurrences of analcime in the Green River Formation (modified according to Remy and Ferrell, 1989) [14, 54, 63–69].

Location	Stratigraphic	Lithology	Proposed origin	References
Utah	Colorado and Parachute Creek Mbr	Oil shale, tuff, and marlstone	Siliceous glass or clay ⟶ zeolite precursor ⟶ analcime	Cole and Picard [14]
Utah, Colorado, Wyoming	Upper Green River Formation	Oil shale and tuff	Dissolution products of siliceous glass + salts in lake ⟶ analcime	Bradley [54]

Table 3: Continued.

Location	Stratigraphic	Lithology	Proposed origin	References
Colorado	Parachute Creek Mbr.	Oil shale and tuff	Siliceous glass ⟶ precursor clays and zeolites ⟶ analcime	Brobst and Tucker [64]
Colorado	Parachute Creek Mbr.	Oil shale, tuff, and marlstone	Siliceous glass ⟶ precursor clays and zeolites ⟶ analcime	Brobst and Tucker [65]
Wyoming	Laney Mbr.	Oil shale, tuff, and tuffaceous sandstone	Siliceous glass ⟶ montmorillonite clino ⟶ ptilolite and mordenite ⟶ analcime	Roehler [66]
Wyoming	Tipton Shale Mbr.	Tuff	Siliceous glass ⟶ alkali zeolites ⟶ analcime	Goodwin and Surdam [67]
Wyoming Mbr., Laney Mbr.	Upper Wilkins Peak Mbr. and Upper Tipton Shale	Tuff	Siliceous glass ⟶ precursor zeolite ⟶ analcime	Iijima and Hay [68]
Wyoming	Laney Mbr.	Tuff	Siliceous glass ⟶ precursor zeolite + upwelling Na-carbonate brine ⟶ analcime	Ratterman and Surdam [69]

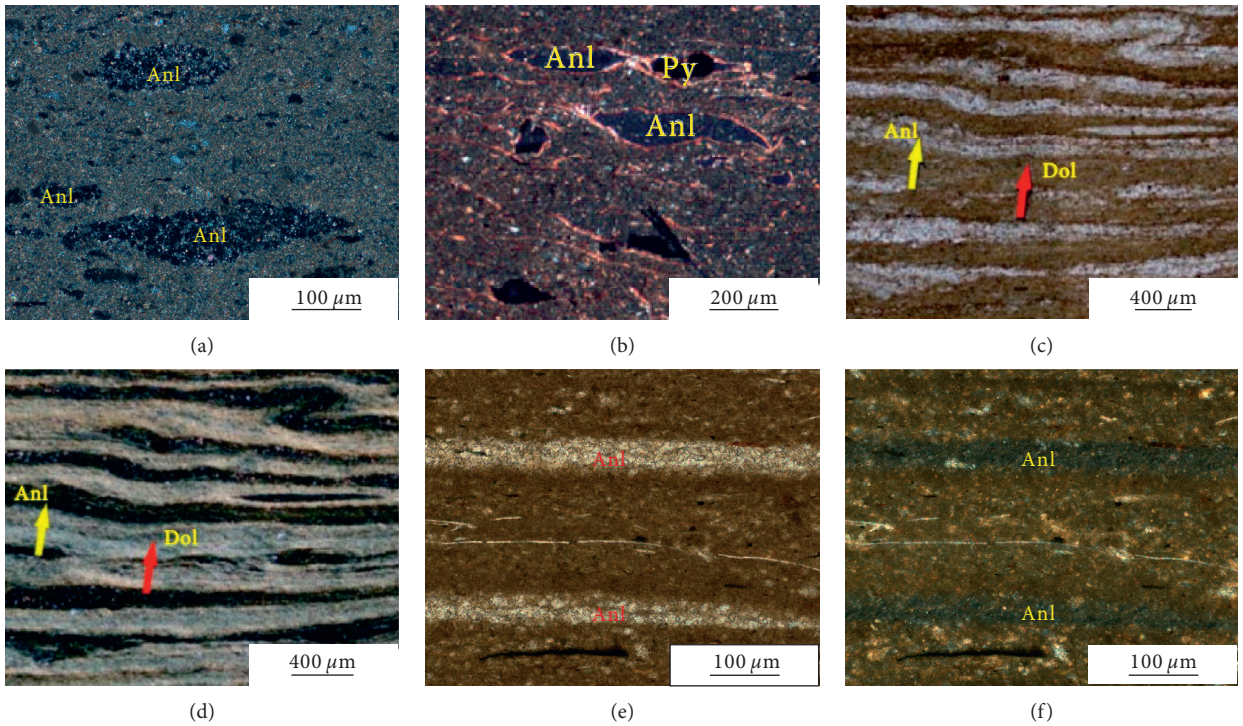

Figure 8: Analcime transformed from clay minerals. (a) Analcime aggregation is lenticular. (b) The interference color of the matrix is affected by dispersed calcite micrite and the entire matrix is dark [19]. (c, d) Microcrystalline analcime and microcrystalline dolomite are thinly interbedded [8]. (e, f) Microcrystalline analcime is interbedded with clay layers and mixed layers.

3.2.2. Feldspar Transformation. The analcime formed by feldspar transformation is mainly distributed in places where the clastic particles are enriched. This type of analcime has an obvious clastic particle profile (Figure 9). Distinguished from quartz and feldspar, analcime showed the characteristics of low-negative projections under single polarized light and full extinction under orthogonal light. Feldspar converts to analcime following two modes [29]: (1) feldspar–feldspar exchange or (2) feldspar–sodium-rich fluid exchange. In feldspar–feldspar mode, active ion exchange between potassium feldspar and albite-rich feldspar in an alkaline environment provides favorable conditions for forming analcime. In feldspar–sodium-rich fluid mode, potassium feldspar and albite-rich feldspar react with the fluid and metal cations, such as Na^+ and Al^{3+}, enter the silicate–aluminate lattice structure through ion exchange, and eventually form analcime. For the analcime formed

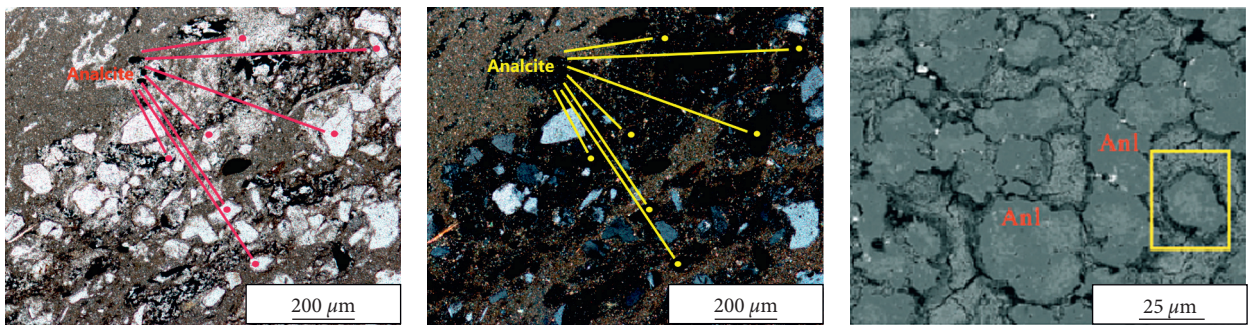

Figure 9: Analcime transformed from feldspar. (a, b) Analcime formed by conversion of K-feldspar. (c) The metasomatism remnant orthoclase can be seen inside the analcime [20].

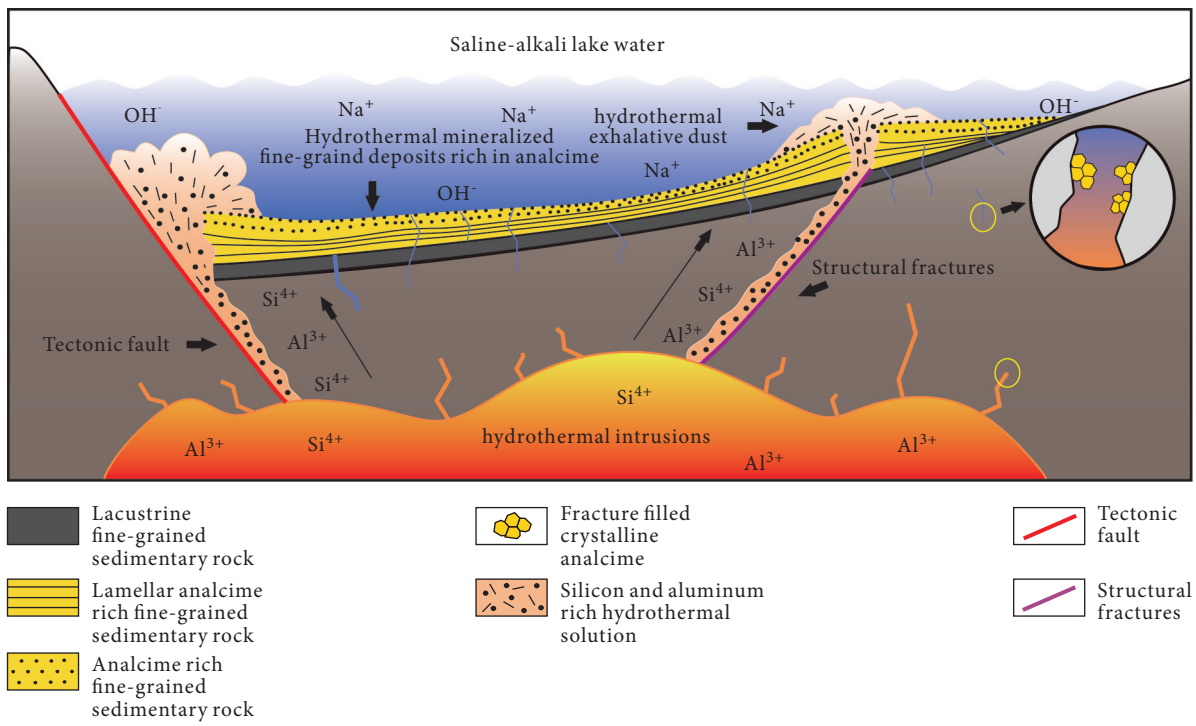

Figure 10: Schematic of hydrothermal sedimentary mineralization of analcime (modified according to Su et al., 2019) [70].

from feldspar, the negative correlation is obviously between alkaline feldspar and analcime.

$$2\mathrm{KAlSi3O_8\,(potassium\,feldspar)} + 4\mathrm{NaOH} = \mathrm{Na_2[AlSi_2O_6]_2 \cdot 2H_2O\downarrow} + \mathrm{Na_2SiO_3} + \mathrm{K_2SiO_3}, \quad (5)$$

$$2\mathrm{NaAlSi_3O_8\,(albite)} + 4\mathrm{NaOH} = \mathrm{Na_2[AlSi_2O_6]_2 \cdot 2H_2O\downarrow} + 2\mathrm{Na_2SiO_3}. \quad (6)$$

3.3. Hydrothermal Deposition Mineralization: H Type. Analcime formed via hydrothermal deposition mineralization often occurs in carbonate layers and is closely related to chemical deposition. According to previous studies, analcime can be divided into two formation mechanisms: (1) reaction between upwelling hydrothermal fluid and sodium-rich alkaline water and (2) transformation of alkali-based silicate–aluminate gel.

The resulting analcime formation is laminar and fissure filling (Figure 10). When the upwelling hydrothermal fluid directly reacts with sodium-rich alkaline water, the associated analcime usually shows laminar distribution

(Figures 11(a) and 11(b)). If the fluid only migrates along fractures, the analcime commonly forms as fissure filling (Figures 11(c) and 11(d)) [23, 34]. In the dolomite of the Es_3, Beitang Sag, Bohai Bay Basin, a large number of fissure-filling analcimes are developed with a small amount of barite and pyrite (Figures 11(e)–11(h)) [8]. In the Paleogene sedimentary rocks of the Es_4 member of the Shahejie Formation in the Western Depression, hydrothermal sedimentary structures and pyrites were deposited simultaneously, indicating the genesis of analcime [9].

Analcime formed by the conversion of alkali–silicate–aluminate gel is usually amorphous (Figure 11(i)). At shallow depths, lake water infiltrates into the strata along the cracks. When the water meets with upwelling hydrothermal fluid, high-pressure steam is formed to eject magma, crystallized volcanic glass, and surrounding rock debris into the lake [25, 29]. The great pressure of the steam crushes the solid components of the mixed hydrothermal fluid, and these eventually migrate to the bottom of the lake in the form of muddy–silty-grained turbidite currents. Because of the thermal repulsion between the particles, the formation and precipitation of aggregate are difficult. Therefore, analcime moves away from the jet point and eventually forms a silica–aluminum-rich fine-grained sedimentary layer [25, 71]. In the later stage, laminar analcime was formed under the reaction dominated by sodium-rich alkaline lake water.

3.4. Precipitated Directly by Alkaline Lake or Pore Water: P Type. Analcime formed via direct precipitation of alkaline lake or pore water usually has the following characteristics [27, 28]: (1) great crystal morphology, (2) pure uniformity, and (3) no metasomatic structure. In the Triassic Lockatong Formation in Pennsylvania and New Jersey, analcime is formed by the recombination of clay minerals and aluminosilicate gels [26]. In the Rocky Brook Formation of the Deer Lake Basin, analcime is formed by direct precipitation of sodic lake or pore fluids [7, 27]. Previous studies have pointed out that P-type analcime usually distributed in three forms: (1) continuous lamina (Figure 12(a)); (2) discontinuous lenticular lamina (Figure 12(b)); (3) equine crystal particle (Figure 12(c)). For sources, the enrichment of analcime is usually closely related to volcanic events, hydrothermal activities, and the climate related to the salinization of the lake basin. Under the action of volcanic events, the tuffaceous matter has become an important part of sediments, and under the control of the transverse salinity of the lake water, its metamorphic products are distributed in a circular band in the lake (Figure 6). Under the action of hydrothermal activities, analcime often fills the channel of hydrothermal upwelling with barite, pyrite, and other hydrothermal minerals. If analcime is formed under the influence of climate, it often presents the interbedding with adjacent layer composition regularly (Figures 12(d) and 12(e)).

4. Reservoir Response

In 1928, Bradley reported the first case of authigenic analcime in the tuff and oil shale of the Eocene Green River Formation in North America. Because of the obvious effect of analcime on reservoir transformation, it has received special attention in developing oil-bearing basins. Its distribution, genesis, and changes in reservoir properties have become major issues for domestic and foreign scholars. Highly coincidental characteristics of analcime-rich areas and shale oil sweet spots are reported in the Green River Formation oil shale in Utah [14, 19, 54, 66, 72], fine-grained sedimentary rocks of the Cangdong Depression in the Bohai Bay Basin [19], and the dense reservoirs in the Jimusar Depression of the Junggar Basin [12, 20]. In these cases, porosity usually increases with the increase of analcime content (Figure 13), which indicates the importance of analcime for shale oil and gas exploration.

4.1. Mechanism of Increasing Porosity. Among common clastic rock autogenetic minerals, analcime has a relatively small specific gravity and large lattice cavity, which make absorbing and filtering other substances of different molecules possible (Department of Geology, Department of Rock and Mineralogy, Peking University, 1979). The compression resistance of analcime is greater than that of carbonate and sulfate minerals. Precipitation in alkaline environments and dissolution in acidic environments is simple, and the pH of its precipitation environment is 8–10. Under the same conditions, the seepage provided by the analcime cementation phase is greater than that of carbonate and sulfate cementation.

Analcime mainly increases secondary pores through the process of precipitation–dissolution to increase the reservoir space for oil and gas (Figure 14). Fine-grained sedimentary reservoirs mainly comprise clay minerals, argillaceous or silty silica particles, and micritic carbonate particles, including oxides, halides, organic matter, and bioclastics. Among them, clay minerals and siliceous minerals are often used as the source minerals of analcime in high-salinity alkaline water environments. In the syngenetic shallow burial stage dominated by sedimentary water, N-type and V-type analcime are formed. In the syngenetic stage, the sediments still directly contact the sedimentary water body and lamellar analcime is directly precipitated by the alkaline lake or pore water on the contact surface. In the penecontemporaneous stage, the sediments are basically separated from the sedimentary water, which is manifested as the direct precipitation of the seeping lake water in the mineral particle pores, bioclastic body cavities, or shielding spaces to form the filling-type analcime. During active tectonic periods, hydrothermal fluids increase along the fractures or faults with large amounts of Si^{4+} and Al^{3+}. When the hydrothermal fluid directly contacts and mixes with the sedimentary water body, an analcime-rich carbonate layer is formed with the jet point as the center. If the hydrothermal fluid does not enter the sedimentary water, filling-type

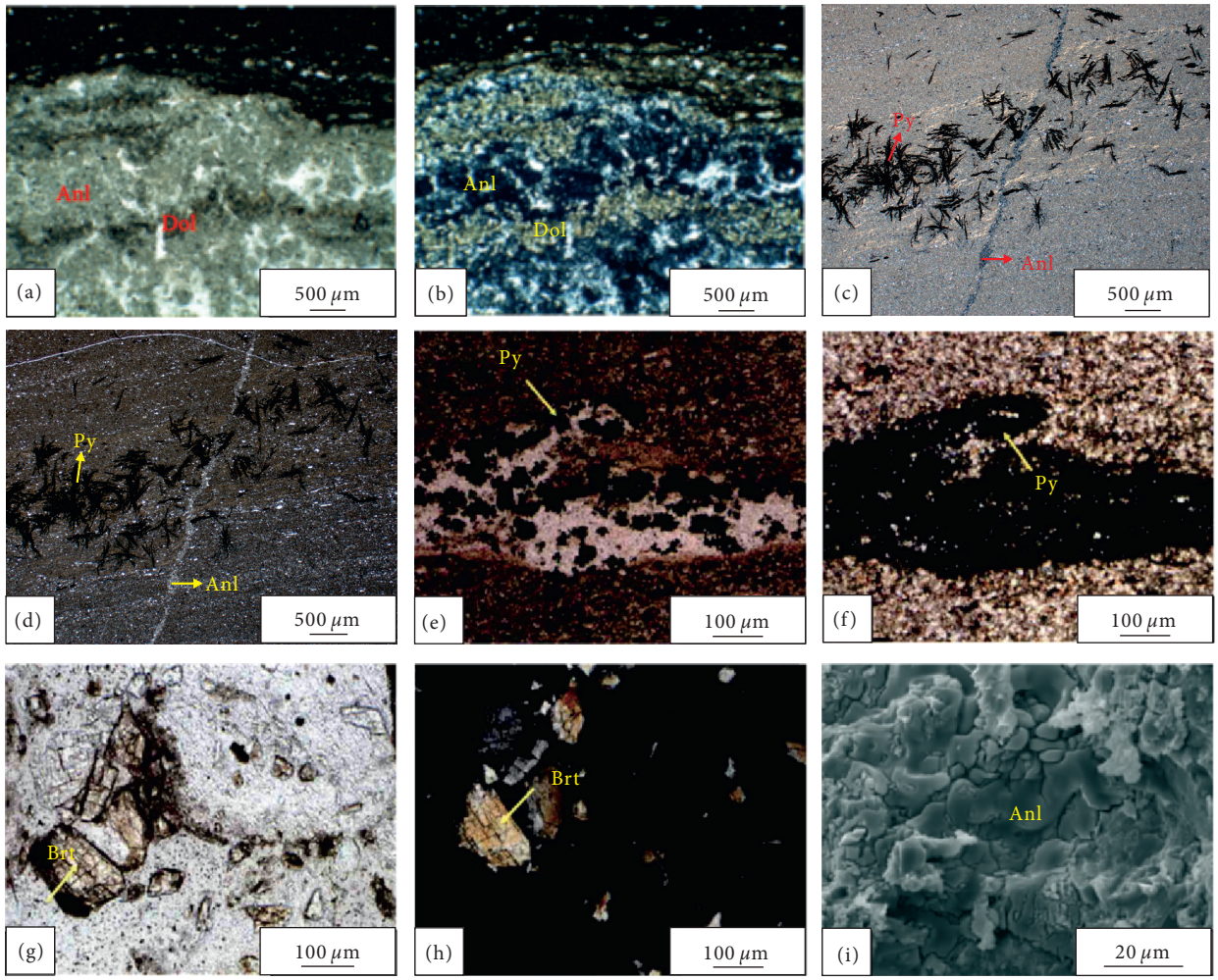

Figure 11: Analcime formed by hydrothermal deposition mineralization. (a, b) Analcime enriched in laminae and interbedded with dolomite [20]. (c, d) Interbedded fractures are filled with hydrothermal analcime. (e, f) Pyrite and analcime distributed in dolomite fractures [8]. (g, h) Analcime filling the fractures is accompanied by barite [8]. (i) Amorphous analcime [23].

analcime is formed by the mixture of sodium-rich alkaline pore water and hydrothermal fluids.

When the source rock enters the intermediate diagenesis stage, massive organic acids are generated, and numerous secondary pores are formed by the dissolution of analcime, which provides favorable conditions for the accumulation of oil and gas. When the adjacent source rocks enter the diagenetic stage of organic matter maturity, an organic–inorganic reaction diagenetic system will be formed in the syngenetic and early diagenetic stage [74], resulting in a high-quality secondary reservoir related to analcime (Figure 15). In the intermediate diagenetic stage, fluid fracturing, dissolution of carbonate, and feldspar influenced by the acidic fluid are important mechanisms to increase the porosity in fine-grained reservoirs.

4.2. Mechanism of Decreasing Porosity. Pore reduction can be divided into two types: physical and chemical pore reductions. Physical pore reduction involves the destruction of a primary intergranular skeleton space and is caused by mechanical compaction before the complete consolidation of sediment. Chemical pore reduction is mainly caused by mineral cementation. During the penecontemporaneous and early diagenetic A stage, the sediment is frequently exchanged with saline-alkaline water, forming alkaline mineral precipitation (e.g., alkaline feldspar and zeolite) that filled the fractures and grain skeletons. In the early diagenetic B stage and intermediate diagenetic A stage, liquid hydrocarbon is generated from kerogen and numerous microfractures are formed in mud shale under the effect of high pressure caused by hydrocarbon generation. Acidic fluid moves along the fracture pores to dissolve the alkaline minerals formed earlier and massive primary carbonate develops and cements along the skeleton grains. Entering the stage of condensate gas generated by thermal cracking in the intermediate diagenetic B stage, the content of organic acids decreases, diagenetic fluid changes from acid to alkaline, and the dissolution of alkaline minerals becomes weak. From the aforementioned discussion, in the sediment consolidation stage, physical and mechanical compaction is the main

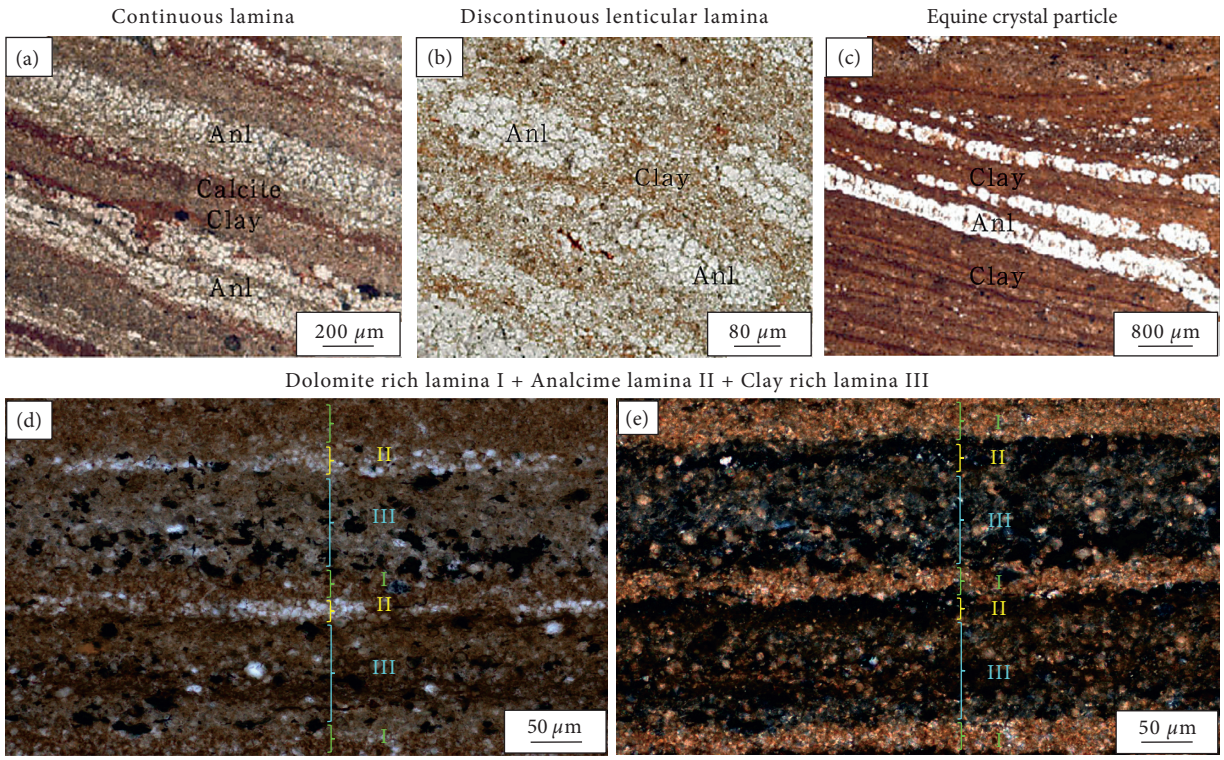

FIGURE 12: Analcime formed by precipitation from the alkaline lake or pore water. (a) Continuous lamina analcime [19]. (b) Discontinuous lenticular lamina analcime [19]. (c) Equine crystal particle analcime [19]. (d, e) Analcime distributed in a fixed pattern with other adjacent lamina.

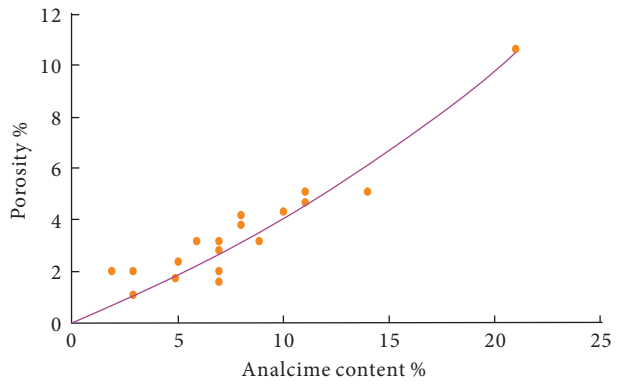

FIGURE 13: Relationship between analcime content and reservoir porosity [12, 20].

mechanism of pore reduction, and with increasing burial depth, ground temperature, and maturity of organic matter, fluid chemistry plays a dominant role instead in reducing porosity. The pore reduction involving analcime includes the precipitation of alkaline minerals formed during the syngenetic and early diagenetic periods and alkaline cementation formed by the transition from acid to alkaline during the intermediate diagenetic B stage.

The discussion above indicates that analcime experienced a complex transformation in the process of diagenesis and hydrocarbon generation. To better understand the genesis and chemical changes of analcime, discussing the reservoir structure, material composition, and volcanic and hydrothermal activities is necessary, especially the sealing adjustment and organic–inorganic synergistic process in the diagenetic process hydrocarbon source rock. Overpressure is

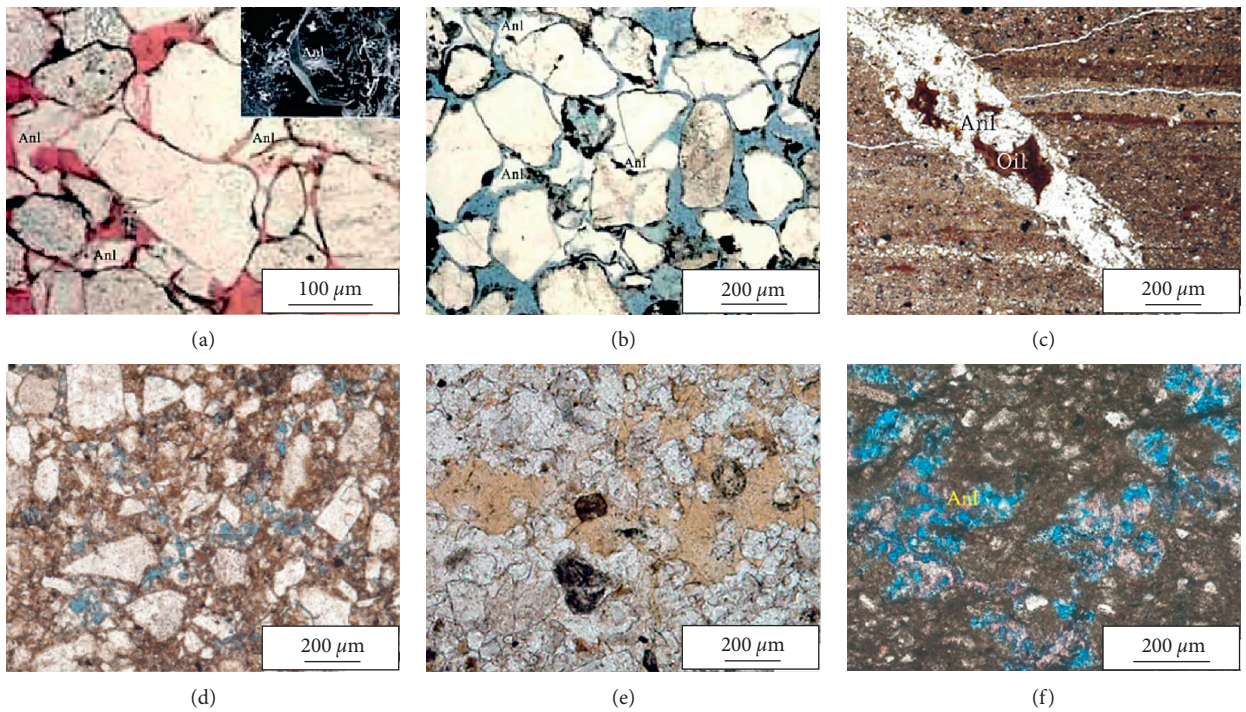

FIGURE 14: Secondary solution pores of analcime under the precipitation-dissolution mechanism. (a) Intergranular analcime is dissolved and pores are shown in red; the inset shows the corrosion characteristics of analcime under an electron microscope [73]. (b) Intergranular analcime is dissolved and pores are shown in blue [73]. (c) A crack in the layers is filled by analcime and oily asphalt [19]. (d) Analcime dissolution pores in silty sandstone [19]. (e) Secondary pores are formed by strong cementation and local dissolution of sparry analcime in siltstone [19]. (f) Dissolution pores of analcime are developed [20].

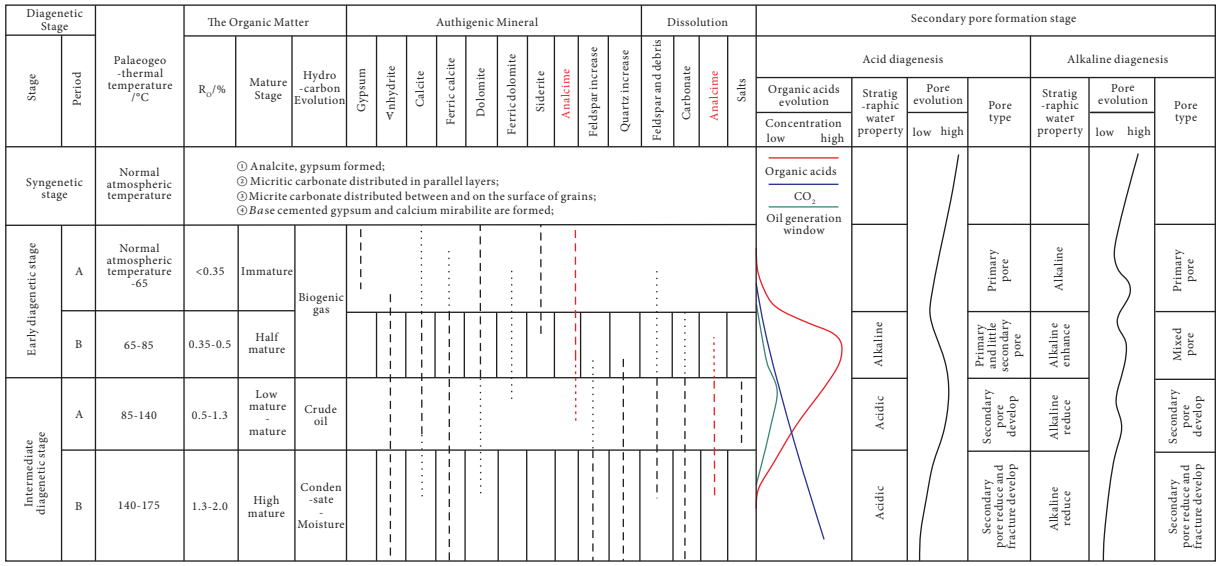

FIGURE 15: Relationships among precipitation-dissolution of analcime and the diagenesis stage of clastic rocks in alkaline water (modified according to Sun et al., 2014) [74].

common in shale. The cementation of calcite is restrained in the overpressure layer while strongly occurring at the interface between the overpressure layer and atmospheric pressure layer, which is due to the influence of pressure and pore size on the crystallization concentration. It is unclear whether a similar effect can also be used as one of the formation mechanisms of lamellar analcime; therefore, the discussion of analcite should not exist independently but should be incorporated into the discussion of mudstone diagenesis.

5. Conclusions

This article summarizes the methods for identifying the source of analcime distributed in fine-grained sedimentary rocks in petroliferous basins. It expounds on analcime occurrence characteristics, formation mechanisms, and diagenetic stages, analyzes its impact on reservoir properties; and summarizes the optimal type of reservoir property transformation. The summary and analysis results are as follows:

(a) The basis for judging the source of analcime mainly includes four aspects: (1) the occurrence form of analcime; (2) minerals associated with analcime and their relative contents; (3) geochemical characteristics; (4) Si/Al ratio. The occurrence location, particle size, automorphism, purity, and fracture development of analcime can indicate the source of analcime macroscopically. The correlation between the enrichment of associated minerals and the content of analcime indicates that it may provide a material source for the formation of analcime or effectively improve the formation environment of analcime. Geochemical data are often used to identify analcime related to primary magmatic crystallization and hydrothermal processes and the genetic source grouping scheme based on the Si/Al ratio, which is a traditional means to identify the source of analcime, has been widely used in the research process of analcime.

(b) There are four main formation mechanisms of analcime in fine-grained sedimentary rocks: (1) burial alteration of volcanic materials (V-type); (2) conversion of nontuffaceous materials (N-type); (3) hydrothermal deposition mineralization (H-type); (4) precipitated directly by the alkaline lake or pore water (P-type).

(c) In the fine-grained sedimentary reservoirs of petroliferous basins, V-type, N-type, P-type, and H-type analcime formed before the organic acid release stage of the source rocks can effectively improve the reservoir properties through a precipitation–dissolution mechanism. Because of the strong compaction resistance, analcime formed from the penecontemporaneous to early diagenetic stage retains some reservoir space in the intermediate diagenetic B stage and late diagenetic periods. When the source rocks release massive organic acids, the early formed analcime is dissolved to form secondary pores. Pore reduction involving analcime includes the precipitation of alkaline minerals formed in the syngenetic and early diagenetic periods and alkaline cementation formed by the transition from acidic to alkaline conditions during the intermediate diagenetic B stage.

(d) Analcime experienced a complex transformation in the process of diagenesis and hydrocarbon generation; possible important factors include the content of organic matter and the adjustment of mineral composition and sealing condition.

Conflicts of Interest

The authors declare that they have no conflicts of interest.

Acknowledgments

The research presented in this article was supported by the National Natural Science Foundation of China (nos. 42072164, U1762217, 41821002, and 41702139), Taishan Scholars Program (no. TSQN201812030), the Fundamental Research Funds for the Central Universities (19CX07003A), and Shandong Provincial Key Research and Development Program (2020ZLYS08).

References

[1] W. H. Bradley, "Zeolite beds in the Green River formation," *Science*, vol. 67, no. 1725, pp. 73-74, 1928.

[2] L. H. Richard, *Zeolites and Zeolitic Reactions in Sedimentary Rocks*, pp. 1–85, Geological Society of America, INC, New York, NY, USA, 1966.

[3] D. S. Coombs and T. Whetten, "Composition of analcime from sedimentary and burial metamorphic rocks," *The Geological Society of America Bulletin*, vol. 8, no. 2, pp. 265–279, 1967.

[4] R. C. Surdam and H. P. Eugster, "Mineral reactions in the sedimentary deposits of the Lake Magadi region, Kenya," *The Geological Society of America Bulletin*, vol. 87, no. 12, pp. 1739–1752, 1976.

[5] S. Zhu, X. Zhu, X. Wang, and Z. Liu, "Zeolite diagenesis and its control on petroleum reservoir quality of Permian in northwestern margin of Junggar Basin, China," *Science China Earth Sciences*, vol. 55, no. 3, pp. 386–396, 2012.

[6] Q. Gall and R. N. Hiscott, "Diagenesis of locally uraniferous sandstones of the Deer Lake group, and sandstones of the Howley formation, carboniferous Deer Lake subbasin, western newfoundland (Canada)," *Bulletin of Canadian Petroleum Geology*, vol. 34, no. 1, pp. 17–29, 1986.

[7] Q. Gall and R. Hyde, "Analcime in lake and lake-margin sediments of the carboniferous Rocky Brook Formation, western newfoundland, Canada," *Sedimentology*, vol. 36, no. 5, pp. 875–887, 1989.

[8] P. X. Lin, C. Lin, Y. Yao et al., "Characteristics and causes of analcime distributed in dolostone of the member 3 of Paleogene Shahejie formationin Beitang sag, Bohai Bay Basin," *Journal of Palaeogeography*, vol. 19, no. 2, pp. 241–256, 2017.

[9] R. Fang, Z. Y. Dai, Z. J. Chen, J. F. Shan, K. Jin, and Y. F. Zhang, "Characteristics and genesis of analcime in different occurrence states: a case study of the fourth member of Shahejie Formation in Leijia area, western sag, Liaohe depression," *Acta Mineralogica Sinica*, vol. 40, no. 6, pp. 88–100, 2020.

[10] R. R. Remy, "Distribution and origin of analcime in marginal lacustrine mudstones of the Green River formation, south-central uinta basin, Utah," *Clays and Clay Minerals*, vol. 37, no. 5, pp. 419–432, 1989.

[11] M. W. Taylor and R. C. Surdam, "Zeolite reactions in the tuffaceous sediments at Teels marsh, Nevada," *Clays and Clay Minerals*, vol. 29, no. 5, pp. 341–352, 1981.

[12] P. M. English, "Formation of analcime and moganite at Lake Lewis, central Australia: significance of groundwater evolution in diagenesis," *Sedimentary Geology*, vol. 143, no. 3-4, pp. 219–244, 2001.

[13] A. Roy and M. Z. Haider, "Stern review on the economics of climate change," *South African Journal of Economics*, vol. 75, no. 1, pp. 369–372, 2006.

[14] R. D. Cole and M. D. Picard, "Comparative mineralogy of nearshore and offshore lacustrine lithofacies, parachute creek member of the Green River formation, piceance creek basin, Colorado, and eastern uinta basin, Utah," *The Geological Society of America Bulletin*, vol. 89, no. 10, pp. 1441–1454, 1978.

[15] R. A. Sheppard, *[Studies in Surface Science and Catalysis] Zeolites: Facts, Figures, Future Part A-Proceedings of the 8th International Zeolite Conference*, Elsevier, Zeolitic Alteration of Lacustrine Tuffs, Western Snake River Plain, Idaho, USA, 1989.

[16] D. Savage, C. Walker, R. Arthur, C. Rochelle, C. Oda, and H. Takase, "Alteration of bentonite by hyperalkaline fluids: a review of the role of secondary minerals," *Physics and Chemistry of the Earth*, vol. 32, no. 1-7, pp. 287–297, 2007.

[17] M. D. Campo, C. D. Papa, J. Jiménez-Millán, and F. Nieto, "Clay mineral assemblages and analcime formation in a Palaeogene fluvial–lacustrine sequence (Maíz Gordo Formation Palaeogen) from northwestern Argentina," *Sedimentary Geology*, vol. 201, no. 1-2, pp. 56–74, 2007.

[18] N. Karakaya, M. Ç. Karakaya, and A. Temel, "Mineralogical and chemical properties and the origin of two types of analcime in SW Ankara, Turkey," *Clays and Clay Minerals*, vol. 61, no. 3, pp. 231–257, 2013.

[19] Y. Zhang, S. Y. Chen, Q. A. Meng, J. H. Yan, X. G. Pu, and W. Z. Han, "The discovery of analcite in fine-grained sedimentary rocks of the second member of kongdian formation in Cangdong Sag, Huanghua depression: implications for early digenetic environment," *China Petroleum Exploration*, vol. 20, no. 4, pp. 37–43, 2015.

[20] C. Ma, J. Wang, X. H. Pan, J. Chen, L. Shang, and J. Liu, "Origin and significance of "sweet spots" of analcites in shale oil reservoirs in Permian Lucaogou formation, Jimsar Sag, Junggar Basin," *Petroleum Geology and Experiment*, vol. 42, no. 4, pp. 596–603, 2020.

[21] D. S. Kelley, J. A. Karson, D. K. Blackman et al., "The AT3-60 Shipboard Party, 2001. An off-axis hydrothermal vent field near the Mid-Atlantic Ridge at 30°N," *Nature*, vol. 412, no. 6843, pp. 145–149, 2001.

[22] Y. Q. Liu, H. Li, Y. S. Zhu et al., "Discussion on the genesis of dolomite: permian lacustrine exhalative hydrothermal dolomite was found in Santanghu Basin, Xinjiang," *Acta Sedimentological Sinica*, vol. 30, no. 5, pp. 861–867, 2010.

[23] H. Li, Y. Q. Liu, H. Liang et al., "Origin of lacustrine dolostones of the middle permian Lucaogou Formation in santanghu basin of Xinjiang," *Journal of Palaeogeography*, vol. 14, no. 1, pp. 45–58, 2012.

[24] H. Wen, R. Zheng, H. Qing, M. Fan, Y. Li, and B. Gong, "Primary dolostone related to the cretaceous lacustrine hydrothermal sedimentation in Qingxi sag, Jiuquan Basin on the northern Tibetan plateau," *Science China Earth Sciences*, vol. 56, no. 12, pp. 2080–2093, 2013.

[25] X. Jiao, Y. Liu, W. Yang et al., "A magmatic-hydrothermal lacustrine exhalite from the Permian Lucaogou Formation, Santanghu Basin, NW China - the volcanogenic origin of fine-grained clastic sedimentary rocks," *Journal of Asian Earth Sciences*, vol. 156, pp. 11–25, 2018.

[26] F. Houten, "Crystal casts in upper triassic Lockatong and brunswick formation," *Sedimentology*, vol. 4, 1965.

[27] Q. Gall and R. Hyde, "Analcime in lake and lake-margin sediments of the carboniferous Rocky Brook Formation, western newfoundland, Canada," *Sedimentology*, vol. 36, no. 5, pp. 875–887, 2010.

[28] Y. Bai, Z. X. Li, Q. Zhang, and J. H. Luan, "The review of genetic calssification of analcime," *Western Resources*, vol. 22, no. 6, pp. 54–57, 2016.

[29] S. F. Zhu, H. Cui, Y. Jia, X. M Zhu, H. Tong, and L. C. Ma, "Occurrence, composition, and origin of analcime in sedimentary rocks of non-marine petroliferous basins in China," *Marine and Petroleum Geology*, vol. 113, pp. 104–164, 2019.

[30] T. Armbruster and M. E. Gunter, "1. Crystal structures of natural zeolites," *Natural Zeolites*, vol. 45, no. 1, pp. 1–68, 2001.

[31] L. J. Ferguson and A. D. Edgar, "The petrogenesis and origin of the analcime in the volcanic rocks of the Crowsnest Formation, Alberta," *Canadian Journal of Earth Sciences*, vol. 15, no. 1, pp. 69–77, 1978.

[32] J. F. Luhr and I. S. E. Carmichael, "The Colima volcanic complex, Mexico: Part II. Late-quaternary cinder cones," *Contributions to Mineralogy and Petrology*, vol. 76, no. 2, pp. 127–147, 1981.

[33] Y. Jiang, S. R. Zhao, C. Q. Ma, and J. Y. Zhang, "Characteristics of rock-forming minerals of analcime phonolite in the damxung area, Qinghai-tibet plateau: evidence for primary analcime," *Earth Science - Journal of China University of Geosciences*, vol. 33, no. 3, pp. 320–328, 2008.

[34] R. C. Zheng, H. G. Wen, M. T. Fan, G. X. Wu, and P. F. Xia, "Lithological characteristics of sublancustrine white smoke type exhalative rock of the Xiagou Formation in Jiuxi Basin," *Acta Petrologica Sinica*, vol. 22, no. 12, pp. 3027–3038, 2006.

[35] M. E. Teruggi, "A new and important occurrence of sedimentary analcime," *Journal of Sedimentary Research*, vol. 34, 1964.

[36] P. Xiao, *Mineralogical Research on Cretaceous Analcime in Ordos Basin*, China University of Geosciences, Wuhan, China, 2014.

[37] C. Sanchez-Valle, S. V. Sinogeikin, Z. A. D. Lethbridge et al., "Brillouin scattering study on the single-crystal elastic properties of natrolite and analcime zeolites," *Journal of Applied Physics*, vol. 98, no. 5, Article ID 053508, 2005.

[38] C. Baerlocher, L. B. McCusker, and D. H. Olson, *Atlas of Zeolite Framework Types*, Elsevier, Amsterdam, Netherlands, 2007.

[39] M. Rosenhauer and H. K. Mao, "Studies on the high-pressure polymorphism of analcime by powder X-ray diffraction and differential thermal analysis methods," *Carnegie Institution of Washington Year Book*, vol. 74, pp. 413–415, 1975.

[40] R. M. Hazen and L. W. Finger, "Polyhedral tilting: a common type of pure displacive phase transition and its relationship to analcime at high pressure," *Phase Transitions*, vol. 1, no. 1, 1979.

[41] J. R. Boles, "Synthesis of analcime from natural heulandite and clinoptilolite," *American Mineralogist*, vol. 501, no. 56, pp. 1724–1734, 1971.

[42] A. Iijima, "12. Zeolites in petroleum and natural gas reservoirs," *Natural Zeolites*, vol. 45, no. 1, pp. 347–402, 2001.

[43] D. L. Bish and D. W. Ming, "Reviews in mineralogy & geochemistry: occurrence, properties, applications," *Natural Zeolites*, vol. 45, pp. 1–10, 2001.

[44] D. Savage, C. Rochelle, Y. Moore et al., "Analcime reactions at 25–90°C in hyperalkaline fluids," *Mineralogical Magazine*, vol. 65, no. 5, pp. 571–587, 2001.

[45] S. J. Chipera, F. Goff, C. J. Goff, and M. Fittipaldo, "Zeolitization of intracaldera sediments and rhyolitic rocks in the 1.25 Ma lake of Valles caldera, New Mexico, USA," *Journal of*

Volcanology and Geothermal Research, vol. 178, no. 2, pp. 317–330, 2008.

[46] S. J. Chipera and D. L. Bish, "Rehydration kinetics of a natural analcime," *European Journal of Mineralogy*, vol. 22, no. 6, pp. 787–795, 2010.

[47] A. F. Redkin and J. J. Hemley, "Experimental Cs and Sr sorption on analcime in rock-buffered systems at 250–300°C and Psat and the thermodynamic evaluation of mineral solubilities and phase relations," *European Journal of Mineralogy*, vol. 12, no. 5, pp. 999–1014, 2000.

[48] B. R. Song, H. D. Han, X. D. Cui, X. D. Dong, and J. M. Chen, "Petrogenesis analysis of lacustrine analcime dolostone of the member 4 of Paleogene Shahejie Formation in liaohe depression, Bohai Bay Basin," *Journal of Palaeogeography*, vol. 17, no. 1, pp. 33–44, 2015.

[49] G. Pe-Piper, D. Piper, and J. Nagle, "Scapolite and analcime: monitors of magmatic fluid metasomatism in a major shear zone," *Chemical Geology*, vol. 522, 2019.

[50] E. Varol, "Interpretation of the origin of analcimes with mineralogical, microtextural, and geochemical investigations: a case study from Aktepe region (NE of Kalecik, Ankara, Central Anatolia, Turkey)," *Arabian Journal of Geosciences*, vol. 13, no. 10, pp. 1–10, 2020.

[51] R. C. Zheng, C. S. Wang, L. D. Zhu et al., "Discovery and significance of the first lacustrine "white smoke type" exhalative rock hydrothermal sedimentary dolomite in Jiuxi basin," *Journal of Chengdu University of Technology (Science & Technology Edition)*, vol. 30, no. 1, pp. 1–8, 2003.

[52] C. S. Ross, "Sedimentary analcime," *American Mineralogist*, vol. 13, pp. 195–197, 1928.

[53] C. S. Ross, "Sedimentary analcime," *American Mineralogist*, vol. 13, 1941.

[54] W. H. Bradley, "The occurrence and origin of analcime and meerschaum beds in the Green River formation of Utah, Colorado, and Wyoming," *Survey Professional Paper*, vol. 158a, pp. 1–7, 1929.

[55] D. S. Coombs, *The Nature and Alteration of Some Triassic Sediments from Southland*, New Zealand, 1954.

[56] F. B. Van Houten, "Composition of upper triassic Lockatong argillite, west-central New Jersey," *The Journal of Geology*, vol. 68, no. 6, pp. 666–669, 1960.

[57] W. D. Keller, "Analcime in the Popo Agie member of the chugwater formation," *Journal of Sedimentary Petrology*, vol. 22, p. 7082, 1952.

[58] L. R. High and M. D. Picard, "Sedimentary petrology and origin of analcime-rich Popo Agie member, chug- water (triassic) formation, west-central Wyoming," *Journal of Sedimentary Petrology*, vol. 35, no. 1, pp. 49–70, 1965.

[59] J. Schieber and W. Zimmerle, "The history and promise of shale research," *Shales and Mudstones*, vol. 1998, pp. 1–10, 1998.

[60] A. C. Aplin and J. H. S. Macquaker, "Mudstone diversity: origin and implications for source, seal, and reservoir properties in petroleum systems," *AAPG Bulletin*, vol. 95, no. 12, pp. 2031–2059, 2011.

[61] Z. X. Jiang, C. Liang, J. Wu et al., "Several issues in sedimentological studies on hydrocarbon-bearing fine-grained sedimentary rocks," *Acta Petrolei Sinica*, vol. 34, no. 6, pp. 1031–1039, 2013.

[62] R. W. Renaut, "Zeolitic diagenesis of late Quaternary fluviolacustrine sediments and associated calcrete formation in the Lake Bogoria Basin, Kenya Rift Valley," *Sedimentology*, vol. 40, no. 2, pp. 271–301, 1993.

[63] R. Robert, E. Ray, and Ferrell, "Distribution and origin of analcime in marginal lacustrine mudstones of the green river formation, south-central uinta basin, Utah," *Clays and Clay Minerals*, vol. 37, no. 5, pp. 419–432, 1989.

[64] D. A. Brobst and J. D. Tucker, "Composition and relation of analcime to diagenetic dawsonite in oil shale and tuff in the Green River Formation, Piceance Creek basin, northwestern Colorado," *Journal of Research of the US Geological Survey*, vol. 2, no. 1, pp. 35–39, 1974.

[65] D. A. Brobst and J. D. Tucker, "X-ray mineralogy of the parachute creek member, Green River formation," *The Northern Piceance Creek Basin, Colorado*, vol. 803, p. 53, 1973.

[66] H. W. Roehler, "Zonal distribution of montmorillonite and zeolites in the laney shale member of the Green River formation in the Washakie basin, Wyoming," *Geological Survey Professional Paper*, vol. 800, pp. B121–B124, 1972.

[67] J. H. Goodwin and R. C. Surdam, "Zeolitization of tuffaceous rocks of the Green River formation, Wyoming," *Science*, vol. 157, no. 3786, pp. 307-308, 1967.

[68] A. Iijima and R. L. Hay, "Analcime composition in tuffs of the Green River formation of Wyoming," *American Mineralogist*, vol. 53, pp. 184–200, 1968.

[69] N. G. Ratterman and R. C. Surdam, "Zeolite mineral reactions in a tuff in the laney member of the Green River formation, Wyoming," *Clays and Clay Minerals*, vol. 29, no. 5, pp. 365–377, 1981.

[70] C. Su, D. K. Zhong, P. Qin, and A. Wang, "Mineral precipitation sequence and formation of the lacustrine hydrothermal sediments in the lower cretaceous tenggeer formation in the baiyinchagan sag, China," *Sedimentary Geology*, vol. 398, Article ID 105586, 2019.

[71] J. Trofimovs, R. S. J. Sparks, and P. J. Talling, "Anatomy of a submarine pyroclastic flow and associated turbidity current: July 2003 dome collapse, Soufrière Hills volcano, Montserrat, West Indies," *Sedimentology*, vol. 55, no. 3, pp. 617–634, 2008.

[72] J. W. Smith and C. Milton, "Dawsonite in the Green River formation of Colorado," *Economic Geology*, vol. 61, no. 6, pp. 1029–1042, 1966.

[73] Y. S. Sun, X. N. Liu, Y. Q. Zhang et al., "Analcime cementation facies and forming mechanism of high-quality secondary clastic rock reservoirs in western China," *Journal of Palaeogeography*, vol. 16, no. 4, pp. 517–526, 2014.

[74] C. Liang, Y. C Cao, K. Y. Liu, J. C Wu, and F. Hao, "Diagenetic variation at the lamina scale in lacustrine organic-rich shales: implications for hydrocarbon migration and accumulation," *Geochimica et Cosmochimica Acta*, Article ID S0016703718301686, 2018.